https://doi.org/10.52973/rcfcv-e361810 Revista Científica, FCV-LUZ / Vol. XXXVI

Evaluation of ozonated oil and *centella asiatica* extract on excisional wound healing in Mice

Evaluación del aceite ozonizado y del extracto de *Centella asiática* en la cicatrización de heridas por escisión en ratones

***Eyup Tolga Akyol*[1]*, *Cengiz Ceylan*[1], *Mustafa Usta*[2], *Musa Karaman*[2], *Fatma İlhan*[2], *Muharrem Erol*[1]**

[1]*Balikesir University, Faculty of Veterinary Medicine, Department of Surgery. Cagis Campus, Balikesir, 10145, Türkiye.*
[2]*Balikesir University, Faculty of Veterinary Medicine, Department of Pathology. Cagis Campus, Balikesir, 10145, Türkiye.*
**Corresponding author: etakyol@balikesir.edu.tr*

ABSTRACT

The aim of this study was to evaluate the effects of two topical treatments on wound healing in BALB/c mice: ozonated oil and an *Centella asiatica* extract. On days 3, 7, 14, and 21, the inflammatory response, re–epithelialization, collagen deposition, and the expression of growth factors such as Vascular Endothelial Growth Factor, Fibroblast Growth Factor, and Transforming Growth Factor–beta were assessed in order to evaluate healing. When compared to the control, VetOzon and Madecassol both markedly elevated Transforming Growth Factor–beta and Vascular Endothelial Growth Factor expression in the first phase. By day 7, Madecassol encouraged more advanced re–epithelialization and fibrosis, while VetOzon produced a more marked inflammatory response, which was necessary to start the healing cascade. The superiority of both treatments was evident by day 14, where they achieved complete re–epithelialization, a milestone the control group had not reached. Notably, Madecassol demonstrated significantly higher collagen deposition than both VetOzon and the control on days 14 and 21, indicating superior extracellular matrix synthesis. By day 21, wounds treated with either agent showed advanced remodeling with reduced cellularity and hair follicle regeneration, while control wounds appeared stalled in an earlier healing phase. In conclusion, both agents effectively accelerate cutaneous wound healing, but through complementary pathways. VetOzon acts as an early–phase inflammatory catalyst, making it potentially suitable for chronic or infected wounds, whereas Madecassol functions as a sustained anabolic stimulator, positioning it as an ideal agent for promoting high–quality, regenerative healing in clean wounds.

Key words: *Centella asiatica*; Madecassol; mice; ozone; wound

RESUMEN

El objetivo de este estudio fue evaluar los efectos de dos tratamientos tópicos en la cicatrización de heridas en ratones BALB/c: aceite ozonizado y extracto de Centella asiática. En los días 3, 7, 14 y 21, se evaluaron la respuesta inflamatoria, la reepitelización, la deposición de colágeno y la expresión de factores de crecimiento como el factor de crecimiento endotelial vascular, el factor de crecimiento de fibroblastos y el factor de crecimiento transformante beta para evaluar la cicatrización. En comparación con el grupo control, tanto VetOzon como Madecassol presentaron una expresión marcadamente elevada de factor de crecimiento transformante beta y factor de crecimiento endotelial vascular en la primera fase. Para el día 7, sus mecanismos divergieron claramente: VetOzon indujo una respuesta inflamatoria más pronunciada, esencial para iniciar la cascada de reparación, mientras que Madecassol promovió una reepitelización y fibrosis más avanzadas. La superioridad de ambos tratamientos fue evidente en el día 14, cuando lograron una reepitelización completa, un hito que el grupo de control no había alcanzado. Notablemente, Madecassol demostró una deposición de colágeno significativamente mayor que VetOzon y el control en los días 14 y 21, lo que indica una síntesis superior de la matriz extracelular. Para el día 21, las heridas tratadas con cualquiera de los agentes mostraron una remodelación avanzada con celularidad reducida y regeneración de folículos pilosos, mientras que las heridas de control parecían estancadas en una fase de curación más temprana. En conclusión, ambos agentes aceleran eficazmente la cicatrización cutánea, pero a través de vías complementarias. VetOzon actúa como un catalizador inflamatorio de fase temprana, lo que lo hace potencialmente adecuado para heridas crónicas o infectadas, mientras que Madecassol funciona como un estimulador anabólico sostenido, posicionándolo como un agente ideal para promover una cicatrización regenerativa y de alta calidad en heridas limpias.

Palabras clave: *Centella asiatica*; Madecassol; ratones; ozono; herida

Received: 29/09/2025 Accepted: 27/12/2025 Published: 12/01/2026

INTRODUCTION

The restoration of skin integrity is a highly complex process aimed at repairing damaged tissue, which is achieved through a temporally orchestrated and overlapping cascade of interactions involving numerous cell types and mediators. A thorough understanding of the cutaneous wound healing process, including its key molecular and cellular inflammatory mediators, is essential for the development of effective therapies. Generally, acute wound healing progresses through four distinct yet overlapping phases: hemostasis, inflammation, proliferation, and remodeling [1, 2, 3, 4].

The main objective of the hemostasis phase, which starts after an injury occurs, is to control bleeding. Platelets are activated during this process, and then group together to create the first platelet plug at the site of damage. In addition to stopping the bleeding, this structure acts as a reservoir for a variety of growth factors and cytokines, including Transforming Growth Factor–beta (TGF–β) and Platelet–Derived Growth Factor (PDGF). Additionally, it offers a temporary extracellular matrix (ECM) scaffold for the migration of fibroblasts, keratinocytes, and inflammatory cells [5].

The indications of inflammation at the wound site are caused by vasodilation and increased vascular permeability, which are characteristics of the inflammatory phase. The first cells to arrive are neutrophils, main function is to phagocytose bacteria and cell debris from the wound in order to cleare [6, 7]. Monocytes then differentiate into macrophages, which take over as the most common cell type. In addition to their decontaminating role, macrophages secrete a variety of growth factors and cytokines, including PDGF, TGF–β, Interleukin–1 (IL–1), and Tumor Necrosis Factor–alpha (TNF–α), to initiate the proliferative phase [4, 5, 6].

The proliferative phase is characterized by granulation tissue formation, neovascularization, re–epithelialization, and immunomodulation. Macrophage–derived growth growth factors such as PDGF and TGF–β attract fibroblasts to the wound, ECM synthesis begins, replaces the initial provisional fibrin clot. This matrix initially develops with predominance of Type III collagen, fibronectin, and proteoglycans [7].

The granulation tissue's increased rate of metabolism, which is a feature of the proliferative phase, calls for an adequate supply of oxygen and nutrients. To meet this demand, angiogenesis is initiated by conditions such as Vascular Endothothelial Growth Factor (VEGF). Granulation tissue is the characteristic of this stage, which includes new capillaries and proliferating fibroblasts that synthesize collagen and the new ECM. This is an active scaffold for cell migration, adhesion, proliferation, differentiation, and maturation, and helps in wound contraction [4, 8].

The remodelling phase is characterized by a reorganization of the collagen matrix. The disorganized Type III collagen, synthesized during the proliferative phase, which was synthesized in the proliferative phase, is gradually replaced by Type I collagen with a more organized and stiff architecture. Greater cross–linking between these collagen fibers further enhances the tensile strength of the scar tissue. High concentrations of inflammatory cytokines like TGF–β and mechanical stress induce further maturation and contraction of the wound [4, 5].

Asiaticoside, a major active component of *Centella asiatica*, is known for ability to stimulate proliferation of fibroblasts and ECM synthesis, during the proliferative and remodeling phases of wound healing. Asiaticoside stimulates the expression of Type I and III collagen, components that constitute the structural substrate of wound repair [9].

Moreover, asiaticoside induces angiogenesis. It is also anti–inflammatory, thus inhibiting an extended phase of inflammation. Therapeutic action of asiaticoside, combined with madecassoside—the second most significant compound of the plant with its powerful anti–inflammatory action—is on the basis of a two–way mechanism: on the one side, it induces constructive processes such as fibroplasia, collagen synthesis, and angiogenesis and, on the other side, inhibits excess inflammation [10].

Ozonated oil is a therapeutic strategy that promotes healing by altering the wound microenvironment in a multifaceted way. Medical ozone is an effective antimicrobial agent with broad–spectrum bactericidal, fungicidal, and virucidal properties. When ozone gas is bubbled through oils, it reacts with the unsaturated fatty acids to form therapeutically active compounds, which include ozonides and peroxides [11, 12, 13]. It is also capable of reducing inflammation and pain at the wound site. At low concentrations, reactive oxygen species (ROS) released from the oil activate the body's endogenous antioxidant defense mechanisms. This controlled oxidative signaling stimulates cells within the wound site, triggering the release of endogenous growth factors like PDGF, TGF–β, and VEGF. The resulting increase in the local concentration of these growth factors supports the proliferative phase by stimulating fibroblast proliferation, collagen deposition, and angiogenesis [14, 15, 16, 17].

Furthermore, in acute wounds, it has been demonstrated to histologically enhance the acute inflammatory response—the initial step of wound healing—and improve the cellular response [18].

The aim of this study was to comparatively evaluate the effects of topical asiaticoside and ozonated oil, two agents with distinct mechanisms of action, at the histopathological and immunohistochemical levels.

MATERIALS AND METHODS

Experimental animals and ethical approval

This study was conducted with the approval of the Erciyes University Local Ethics Committee for Animal Experiments (EÜHADYEK) (Approval No: 017/17). A total of 40 adult BALB/c mice (*Mus musculus*), 20 female, 20 male, three months of age and weighing an average of 25–30 grams, were used in this study. Throughout the experimental period, the mice were housed under standard laboratory conditions (22 ± 2°C, 50 ± 5% humidity, a 12–hour (h) light/dark cycle) and provided with *ad libitum* access to standard pellet chow and tap water.

Experimental groups and study design

The mice were randomly assigned to four main groups (n = 10 per group; 5 female, 5 male) based on the euthanasia time point: day (d) 3, d 7, d 14, and d 21. Each animal served as its own control.

Anesthesia and surgical procedure

Anesthesia was induced in an induction chamber with 4% Sevoflurane (Sevorane® 100%, Abbvie, Italy) and an oxygen flow of 1 $L \cdot min^{-1}$. After reaching a surgical plane of anesthesia, the mice were placed in sternal recumbency on an operating table, and anesthesia was maintained with 2% Sevoflurane via a nose cone.

The dorsal region of the animal was shaved, and the surgical site was disinfected with alcohol and Povidone–iodine. On the dorsal midline, three full–thickness excisional wounds were created using a sterile, disposable 4 mm biopsy punch for each wound. Two wounds were created in the cranial region, while the third was positioned approximately 2 cm caudal to the first two. Minor bleeding was controlled with gentle pressure from a sterile gauze pad. Following the procedure, anesthesia was discontinued, and the mice were returned to clean cages.

Wound care and treatment

The three wound sites on each mice were treated as follows:

- **Control Group:** The caudal wound site received no topical agent and was left as the control.
- **Asiaticoside Group:** One of the cranial wounds was treated topically with a thin layer of asiaticoside–containing cream (Madecassol®, Bayer, Switzerland) twice daily.
- **Ozonated Oil Group:** The other cranial wound was treated with a thin layer of ozonated oil (VetOzon, MCY, Türkiye) twice daily.

For postoperative pain management, all mice were administered Metamizole at a dose of 200 $mg \cdot kg^{-1}$ via their drinking water for 3 d following the operation.

Tissue sample collection and fixation

On d 3, 7, 14, and 21, respectively, mice from the corresponding experimental groups were euthanized. Euthanasia was performed by CO_2 inhalation and cervical dislocation. Each wound site, including a 2 mm margin of surrounding healthy skin, was excised as a full–thickness block. The samples were then fixed for 24 h in a 10% neutral buffered formalin solution for subsequent histopathological analysis.

Histopathological examination

On d 3, 7, 14, and 21 of the study, tissue samples obtained from the wound sites of the subjects were fixed in a 10% buffered formalin solution. The fixed tissues were embedded in paraffin blocks, and sections of 5 µm thickness were cut from these blocks using a microtome (RM2245, Leica, Germany). The sections were stained with Hematoxylin and Eosin to observe pathological changes, and with Masson's Trichrome (MT) to determine collagen formation and distribution. The stained sections were then evaluated under a light microscope (Eclipse N*i*, Nikon, Japan). The histopathology score for each case was obtained by summing the criteria detailed [19] in TABLE I.

Immunohistochemical analysis

To identify factors influencing neovascularization and collagen production during wound healing, all samples were stained for VEGF, TGF–β, and FGF using an Avidin–Biotin–Peroxidase Complex method. Five–micrometer (5 µm) thick sections were cut from the paraffin blocks, mounted on poly–L–lysine–coated slides, and allowed to dry overnight in an oven (WiseVen, Wisd, France).

Following deparaffinization, the sections were washed three times in Phosphate–Buffered Saline (PBS) for 5 min each. Subsequently, for antigen retrieval, the slides were incubated (WiseVen, Wisd, France) in a citrate buffer (pH 6.0) for 15 min. After three further washes in PBS, endogenous peroxidase activity was blocked by incubating the sections in 3% hydrogen peroxide for 20 min.

To prevent non–specific binding, the sections were then incubated with a non–immune goat serum for 30 min at room temperature. The sections were subsequently incubated with primary antibodies against VEGF (Abcam, ab1316), TGF–β (Abcam, ab190503), and FGF (Abcam, ab8880) for 1 h at 37°C. After this incubation, sections were washed three times in PBS and treated with a biotinylated secondary antibody for 30 min.

Following another series of washes, the sections were incubated with a peroxidase–conjugated streptavidin complex for 30 min. After a final set of three washes in PBS, the reaction was visualized by applying 3,3'–diaminobenzidine solution as the chromogenic substrate.

TABLE I
Scoring criteria for wound healing

Parameter	0	1	2
Re–epithelialization	No re–epithelialization	Partial re–epithelialization	Complete re–epithelialization
Epidermal thickness index	Hypoplasia	Hypertrophy	Normal
Keratinization	Absent	–	Loosely attached lost/layers or thick parakeratotic stratum corneum
Granulation Tissue	Thick layer of granulation tissue	Thin layer of granulation tissue	No granulation tissue
Remodeling	No collagen synthesis, sebaceous glands, or hair follicle formation	Minimal collagen synthesis; no sebaceous gland or hair follicle formation	Complete collagen synthesis, formation of sebaceous glands and hair follicles
Wound evaluation index	Dermal healing absent/minimal	Hypertrophy of the dermis due to excessive collagen deposition	Dermis is intact and its thickness is consistent with uninjured skin

The reaction was terminated with distilled water as soon as color development was observed. Finally, the sections were counterstained with Mayer's hematoxylin, mounted with Entellan mounting medium, and examined under a light microscope. The quantification of immunopositive areas in the immunohistochemically stained sections was performed using the Fiji digital image analysis software (version 2.12.0).

Statistical analysis

All data obtained from the histopathological and immunohistochemical analyses were statistically analyzed (GraphPad Prism, version 9.5.0). The data were found to be normally distributed. Therefore, a one–way analysis of variance (ANOVA) was performed, followed by Bonferroni's post–hoc test. A *P*–value of less than 0.05 was considered statistically significant.

RESULTS AND DISCUSSION

On d 3 of the study, the Control, VetOzon, and Madecassol groups exhibited similar findings, characterized by intense neutrophilic leukocyte infiltration at the wound margins and the presence of extensive necrotic tissue in the wound bed (FIG. 1 a, b, and c).

Following hemostasis, this period is characterized by an abundance of neutrophilic leukocytes and a smaller population of macrophages in the wound area. These cells decontaminate the wound bed by clearing cellular debris, necrotic tissue, and potential pathogens via phagocytosis, thereby preparing the site for subsequent stages of repair. Towards the end of this phase, neutrophilic leukocytes typically declines [20].

In the present study, on d 3, an intense infiltration of neutrophilic leukocytes, accompanied by edema, fibrin, and extensive necrotic tissue, was observed at the wound margins in all groups. This finding represents the expected and physiologically necessary initial phase of acute cutaneous wound healing. The histopathological similarity observed across all groups on d 3 serves as a crucial internal control, indicating that the initial injury severity was consistent among the groups and that the applied topical agents had not yet induced significant morphological differences.

On d 7, the Control group showed a reduction in necrotic tissue, an increase in inflammatory cell infiltration composed of neutrophils and macrophages, the beginning of partial epidermal regeneration, and mild dermal fibrosis and neovascularization (FIG. 1 d). In the VetOzon group, the inflammatory cell infiltrate of neutrophils and macrophages was notably more severe compared to the Control group, while other findings were similar (FIG. 1e). In the Madecassol group, epithelialization and dermal fibrosis were observed over more extensive areas compared to the Control and VetOzon groups. Neovascularization was also more prominent in this group compared to the other two (FIG. 1f).

By d 7 of the study, the histopathological and molecular differences between the groups had become more pronounced, revealing the distinct mechanism of action for each agent. Towards the end of the inflammatory phase, the number of neutrophilic leukocytes in the wound area decreases, while the population of macrophages and fibroblasts begins to increase. In addition to clearing necrotic tissue and cells, macrophages initiate fibroblast proliferation and the formation of granulation tissue through the growth factors and cytokines they secrete [20].

In the VetOzon group on d 7, the inflammatory cell infiltration, consisting of neutrophils and macrophages, was severe than in the Control group. While this could be interpreted as a pathological response, when evaluated within the framework of ozone's mechanism of action [18], this intense inflammation is thought to form the basis of its therapeutic effect. Ozonated oil reacts

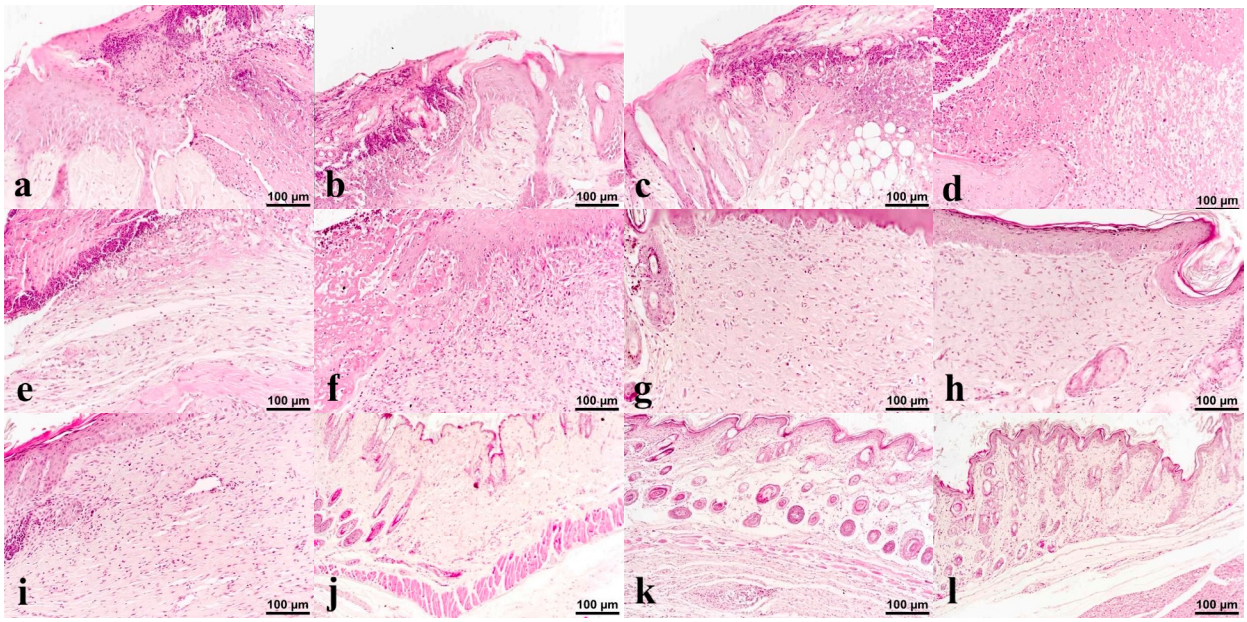

FIGURE 1. Histopathological appearance of the wound healing process. Representative images of the Control (a, d, g, j), VetOzon (b, e, h, k), and Madecassol (c, f, i, l) groups at days 3, 7, 14, and 21 post–wounding. Hematoxylin and Eosin (10×)

with unsaturated fatty acids in the wound bed to form reactive molecules, such as hydroperoxides and aldehydes, known as lipid ozonation products (LOPs).

These LOPs act as signaling molecules by creating a state of controlled acute oxidative stress [21]. The severe migration of neutrophils and macrophages observed in the present study can be explained by this process. Furthermore, it may also promote an increase in growth factors like TGF–β, which are critical for the subsequent stage of healing [22]. Therefore, the intense inflammation induced by VetOzon appears to be the primary mechanism that accelerates the healing cascade and triggers the transition to the proliferative phase. This is further supported by the sustained high expression of TGF–β and the increase in FGF observed in the VetOzon group on d 7.

In contrast, the Madecassol group on d 7 exhibited more extensive epithelialization, along with more prominent dermal fibrosis and neovascularization, compared to the Control and VetOzon groups. This indicates that the primary mechanism of action for Madecassol involves the direct stimulation of keratinocytes and fibroblasts, which are the main cellular actors of the proliferative phase. This effect is attributed to asiaticoside and madecassoside, the active triterpenoid components of *Centella asiatica* [9, 23]. The known ability of these compounds to promote fibroblast proliferation and collagen synthesis was corroborated in the present study by the observed proliferation of the few fibroblasts present in the area and the high expression of TGF–β, FGF, and VEGF. This finding has been interpreted to mean that on d 7, Madecassol facilitates a more rapid transition from the inflammatory to the regenerative phase of wound healing.

On d 14, the Control group exhibited decreased inflammatory cell infiltration, partially complete re–epithelialization, and intense dermal fibrosis; neovascularization in these cases had increased compared to d 7 (FIG. 1 g). In the VetOzon group, inflammatory cell infiltration was reduced, re–epithelialization was complete, and partial maturation of the dermal connective tissue was observed (FIG. 1 h). The Madecassol group showed complete epithelialization and partial maturation of the newly formed dermal connective tissue (FIG. 1 i).

On d 14 of the present study, consistent with the literature, a decrease in inflammatory cell infiltration was observed, alongside the formation of intense dermal fibrosis and neovascularization. Re–epithelialization was observed to be complete in the VetOzon and Madecassol groups, in contrast to the Control group. The reduction in inflammation and the onset of dermal connective tissue maturation in the treatment groups indicate that both agents successfully accelerated the transition from the inflammatory to the proliferative phase. The complete restoration of the epidermal barrier and the resolution of inflammation in the treatment groups point to a functionally superior and more rapid repair process.

On d 21, both the VetOzon and Madecassol groups showed a decrease in inflammatory cells and fibroblasts, with small areas of granulation tissue where new hair follicles were beginning to form. In contrast, the Control group exhibited more abundant granulation tissue and higher cellularity compared to the other two groups (FIGS. 1 j, k, and l).

In the remodeling phase, cellularity decreases through the apoptosis of cells within the granulation tissue, and the tissue transitions to a more metabolically quiescent state [24]. Type III collagen is replaced by the stronger Type I collagen, which imparts tensile strength to the tissue [25]. During this period, vascularity also regresses due to a reduction in angiogenic processes, causing the metabolic activity of the acute wound to slow and eventually cease. On d 21, the final time point of the present study, there was significant differences not only in the speed but also in the quality of healing.

In the VetOzon and Madecassol groups, a marked reduction in cellularity (both inflammatory cells and fibroblasts) and the formation of new hair follicles indicated that the tissue had progressed to an advanced remodeling phase. In contrast, the persistence of highly cellular granulation tissue in the Control group suggested that its healing process was stalled in an earlier phase. The regeneration of adnexal structures, such as hair follicles, is evidence of a regenerative healing model as opposed to simple fibrotic scarring [7]. Therefore, it can be concluded that both treatments not only accelerated wound closure but also promoted the formation of a functionally and aesthetically superior, regenerated tissue.

In the present study, collagen deposition in all cases was evaluated on d 3, 7, 14, and 21 using MT staining. On d 3, no collagen was observed in the wound area of any group (FIG. 2 a, b, and c). On d 7, the amount of collagen had increased in all groups compared to the previous time point, and this increase was observed to be similar across the groups (FIG. 2 d, e, and f). On d 14, the collagen amount was found to be significantly higher in the Madecassol group compared to the Control group ($P<0.05$); however, no significant difference was detected between the VetOzon and Control groups ($P>0.05$) (FIG. 2 g, h, and i). On d 21, the highest amount of collagen was observed in the Madecassol group. The collagen content in this group was significantly greater than in the other two groups ($P<0.05$), while the difference between the Control and VetOzon groups was not statistically significant ($P>0.05$) (FIGS. 2 j, k, and l).

The histopathological scores for the study (TABLE II) and the percentage of collagen–positive areas from the Masson's Trichrome staining are provided in FIG. 3.

The onset of the regeneration period is marked by a gradual decrease in macrophages and the emergence of fibroblasts as the dominant cell type in the healing area [24]. Under the influence of growth factors, granulation tissue—composed of new blood vessels

TABLE II
Comparison of total histopathological healing scores among groups

	Control Group	VetOzon Group	Madecassol Group	*P*–value
Day 3	0.10 ± 0.32	0.10 ± 0.32	0.10 ± 0.32	> 0.05
Day 7	3.40 ± 1.07^{a}	4.60 ± 0.84^{b}	5.30 ± 0.82^{b}	< 0.001
Day 14	4.90 ± 1.29^{a}	6.70 ± 1.16^{b}	7.50 ± 1.08^{b}	< 0.001
Day 21	10.40 ± 1.17	10.70 ± 0.95	11.00 ± 0.82	> 0.05

Different superscript letters (^{a,b}) in the same row indicate statistically significant differences between groups ($P<0.05$). Data are presented as Mean ± Standard Deviation (SD)

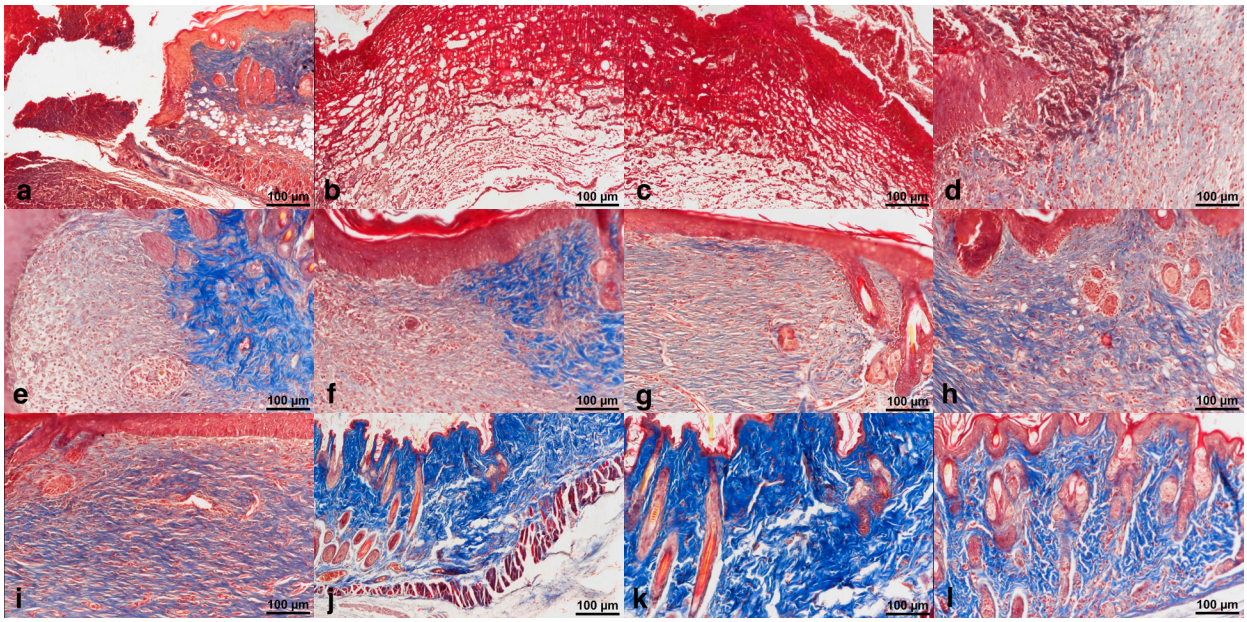

FIGURE 2. Collagen deposition in the wound area evaluated by Masson's Trichrome staining. Representative images of the Control (a, d, g, j), VetOzon (b, e, h, k), and Madecassol (c, f, i, l) groups at days 3, 7, 14, and 21 post–wounding (10×)

and newly synthesized collagen from fibroblasts—is formed. An increase in the number of collagen fibers within the healing region enhances the tissue's strength and resistance [24, 25].

Furthermore, on d 14, collagen deposition in the Madecassol group was greater than in both the Control and VetOzon groups. This superiority continued to d 21, where the collagen amount in the Madecassol group was found to be greater than that of the Control group. The primary mechanism underlying the quantitative superiority of Madecassol is its potent and prolonged stimulation of TGF–β, one of the key molecules in wound healing. Indeed, the present study immunohistochemical findings demonstrated that TGF–β expression remained persistently high in the Madecassol group on d 3, 7, and 14. As a potent pro–fibrotic cytokine, TGF–β directly triggers the synthesis of Type I and III collagen by stimulating fibroblast [26].

These sustained high levels of TGF–β observed in the Madecassol group provided a continuous and robust stimulus for collagen production. This was confirmed by the detection of significantly higher collagen content in the histological analyses on d 14 and 21.

This analysis establishes a direct mechanistic link between the immunohistochemical TGF–β findings and the quantitative collagen data, thereby explaining the superiority of Madecassol in matrix formation. Although VetOzon also increased collagen deposition, this effect was not as pronounced or sustained as that of Madecassol. This result suggests that VetOzon acts as an early–phase modulator that initiates the process, whereas Madecassol acts as a direct and continuous stimulator that supports matrix synthesis mechanisms over a prolonged period.

The results of the immunohistochemical analysis for FGF expression in wound tissues are presented in FIG. 3. On d 3 of wound healing, FGF immunoreactivity was similar across all groups, with no significant difference observed between them ($P>0.05$) (FIGS. 4 a, b, and c). On d 7 (FIGS. 4 d, e, and f) and d 14 (FIGS. 4 g, h, and i), FGF immunoreactivity, observed as intracytoplasmic staining in fibroblasts and macrophages, was significantly higher in both the VetOzon and Madecassol groups compared to the Control group ($P<0.05$). However, the difference in FGF immunoreactivity between the VetOzon and Madecassol groups was not significant ($P>0.05$). By d 21, the levels of FGF immunoreactivity were again similar across all groups ($P>0.05$) (FIGS. 4 j, k, and l).

The lack of a significant difference in FGF expression among all groups in the early (d 3) and late (d 21) stages, contrasted with the observed increase in the treatment groups during the middle phases (d 7 and 14), suggests that FGF primarily plays a role in the intermediate stages of healing. The higher FGF expression in the treatment groups indicates that these therapies not only initiate the proliferative phase but also robustly sustain it. The high levels of FGF observed on d 7 are directly consistent with the early fibroblast proliferation and onset of angiogenesis seen histopathologically. The persistence of this effect to d 14 confirms that granulation tissue formation and tissue remodeling were much more advanced in the treatment groups compared to the Control group.

This sustained high level of FGF suggests that VetOzon and Madecassol keep the wound bed continuously active for repair, thereby laying the groundwork for the superior histological findings observed on d 14, such as complete re–epithelialization and maturing connective tissue. This indicates that both agents accelerate wound healing by effectively utilizing the FGF pathway.

The results of the immunohistochemical analysis for TGF–β expression in wound tissues are presented in FIG. 3. TGF–β immunoreactivity was observed as intracytoplasmic staining in fibroblasts, fibrocytes, and macrophages. On d 3, 7, and 14,

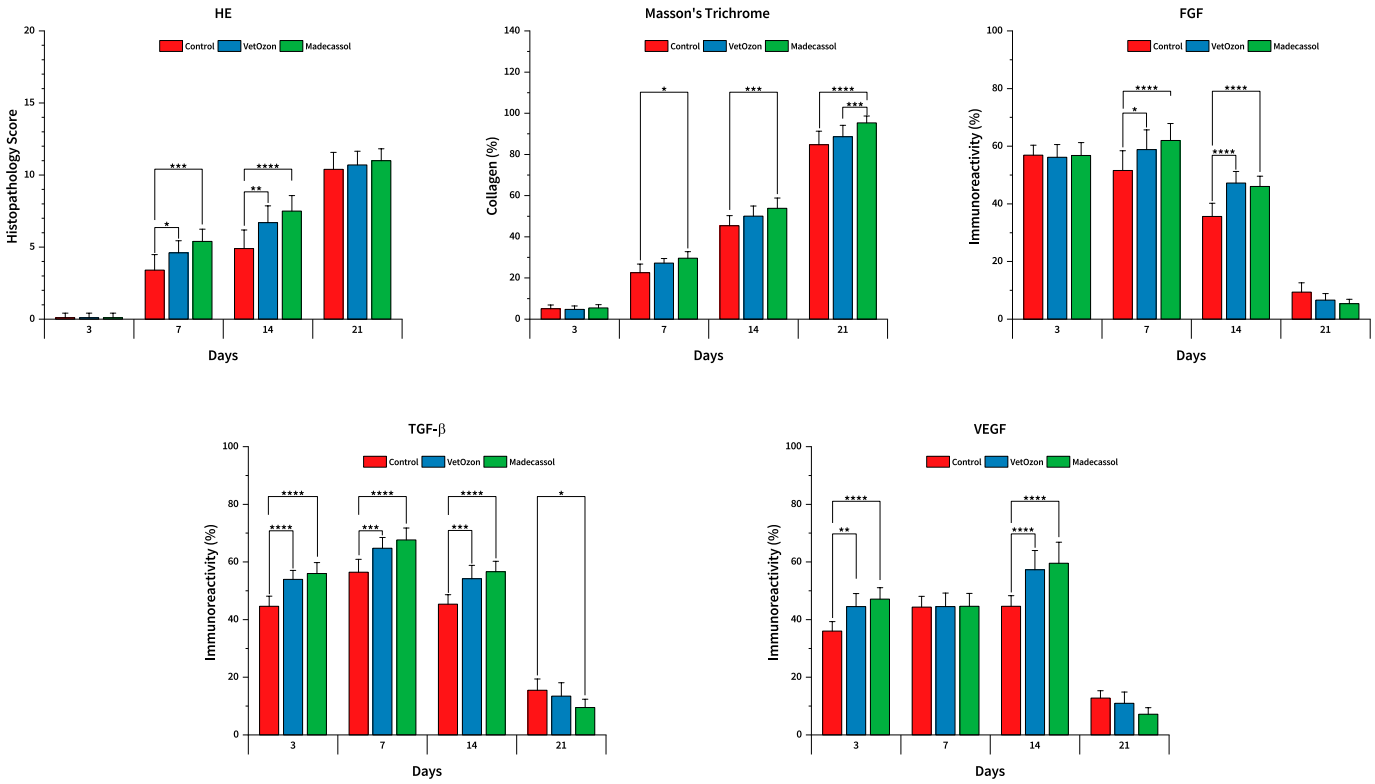

FIGURE 3. Graphical representation of the scores from histopathological and Masson's trichrome staining, and the immunoreactivity of FGF, TGF–β, and VEGF in wound tissues (ns: no significant difference, **P*<0.05, ***P*<0.01, ****P*<0.001, *****P*<0.0001)

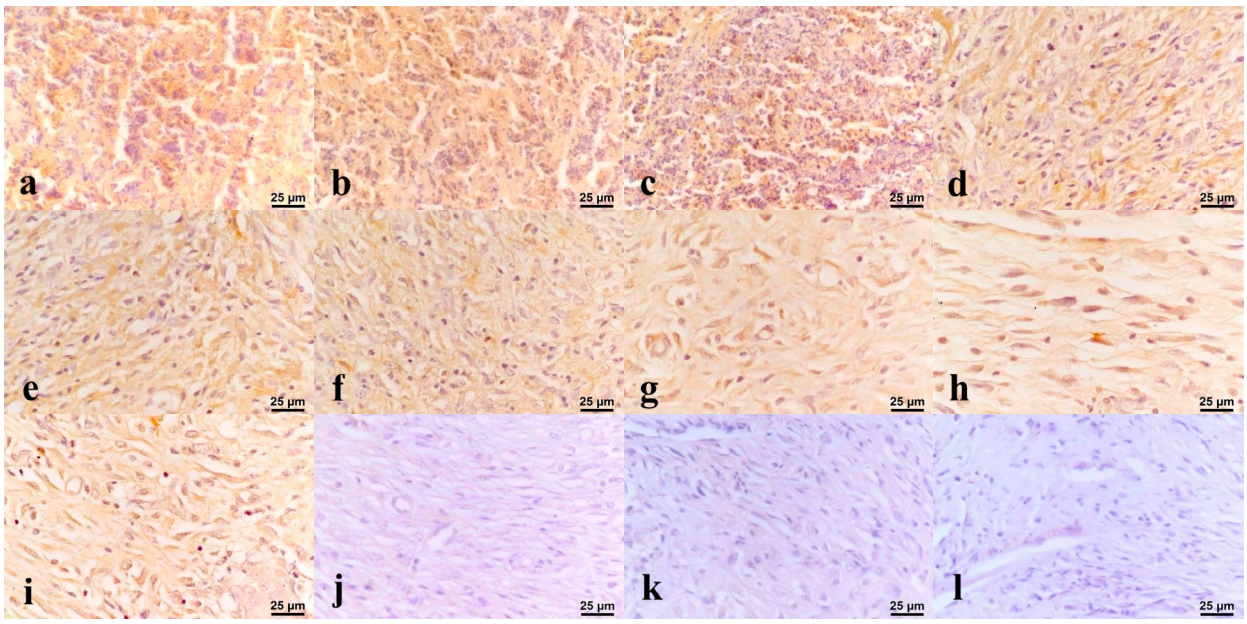

FIGURE 4. Immunohistochemical analysis of FGF expression in wound tissue. Positive intracytoplasmic immunoreactivity is visible in macrophages, vascular endothelial cells, fibroblasts, and fibrocytes. Representative images show the Control (a, d, g, j), VetOzon (b, e, h, k), and Madecassol (c, f, i, l) groups at days 3, 7, 14, and 21 post–wounding (40×)

TGF–β immunoreactivity in both the VetOzon and Madecassol groups was significantly higher ($P<0.05$); however, the difference between the VetOzon and Madecassol groups was not significant ($P>0.05$) (FIGS. 5 a–i). On d 21 of the study, the difference in TGF–β immunoreactivity among the groups was not significant ($P>0.05$) (FIGS. 5 j, k, and l).

The results of the immunohistochemical analysis for VEGF expression in wound tissues are presented in FIG. 3. On d 3 of wound healing, VEGF immunoreactivity in the Control group was significantly lower ($P<0.05$), while no significant difference was observed between the VetOzon and Madecassol groups ($P>0.05$) (FIGS. 6 a, b, and c). On d 7, the levels of VEGF immunoreactivity were similar across all groups ($P>0.05$) (FIG. 6S d, e, and f). On d 14 of the study, VEGF immunoreactivity in the VetOzon and

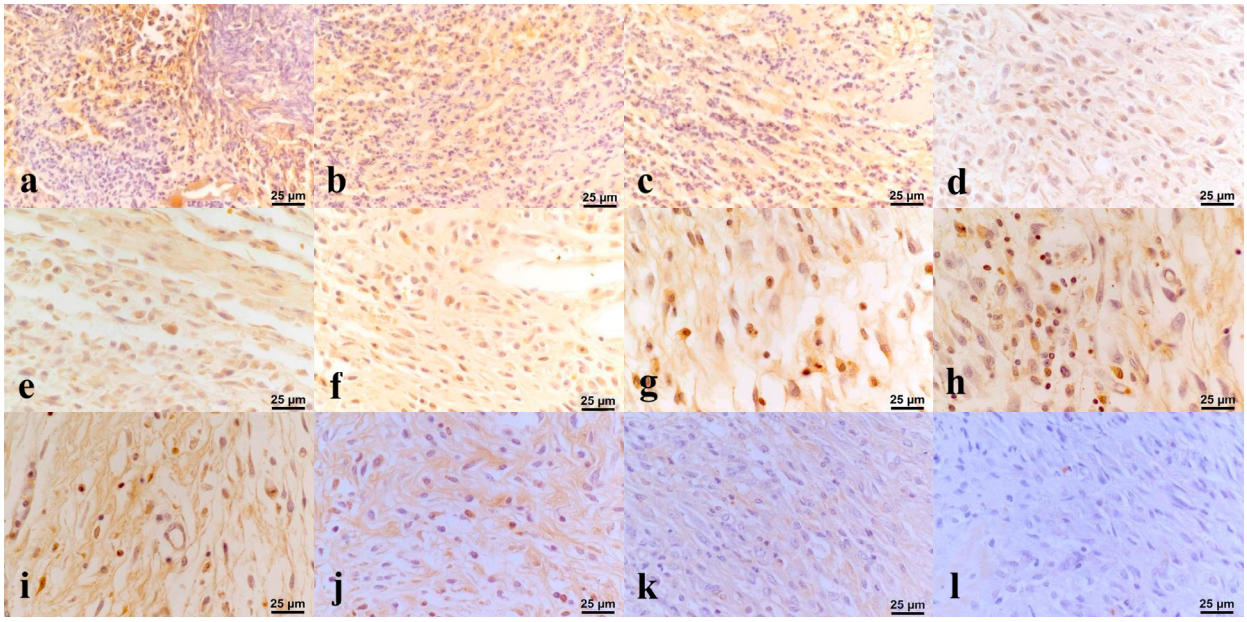

FIGURE 5. Immunohistochemical analysis of TGF–β expression in wound tissue. Positive intracytoplasmic staining is visible in macrophages, vascular endothelial cells, fibroblasts, and fibrocytes. Representative images show the Control (a, d, g, j), VetOzon (b, e, h, k), and Madecassol (c, f, i, l) groups at days 3, 7, 14, and 21 post–wounding (40×)

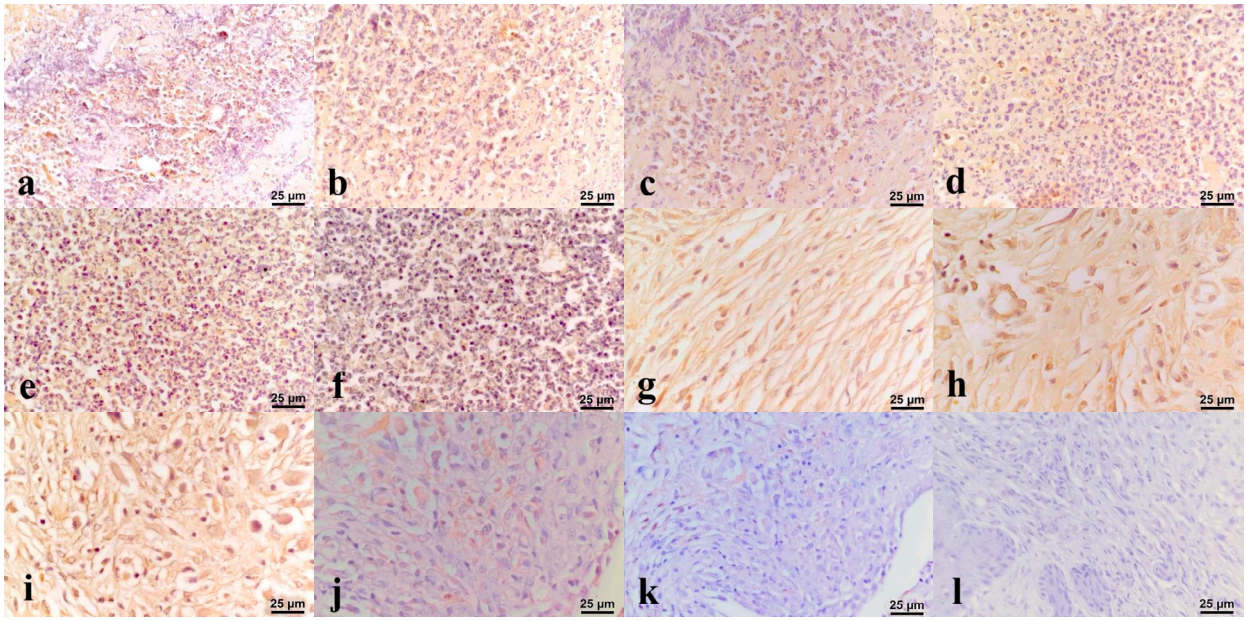

FIGURE 6. Immunohistochemical analysis of VEGF expression in wound tissue. Positive intracytoplasmic staining is visible in neutrophilic leukocytes, macrophages, vascular endothelial cells, fibroblasts, and fibrocytes. Representative images show the Control (a, d, g, j), VetOzon (b, e, h, k), and Madecassol (c, f, i, l) groups at days 3, 7, 14, and 21 post–wounding (40×)

Madecassol groups—observed as intracytoplasmic staining in neutrophilic leukocytes, macrophages, vascular endothelial cells, fibroblasts, and fibrocytes—was significantly higher ($P<0.05$). However, no significant difference between the VetOzon and Madecassol groups ($P>0.05$) (FIGS. 6 g, h, and i). On d 21, VEGF immunoreactivity was again similar across all groups, with no significant difference ($P>0.05$) (FIGS. 6 j, k, and l).

No histopathological differences were observed, by d 3 of the present study findings indicate that significant changes had already commenced at the molecular level. The elevated immunoreactivity for TGF–β and VEGF in the VetOzon and Madecassol groups on d 3 provides the first molecular evidence that these agents prime the wound environment for repair at an early stage. TGF–β, which is released by platelets and early inflammatory cells, is a potent chemoattractant for fibroblasts and other cell types, playing a key role in initiating the proliferative phase [24].

Similarly, VEGF facilitates the transport of nutrients and oxygen to the wound bed by increasing vascular permeability and stimulating angiogenesis [27]. Therefore, the early elevation of these growth factors in the treatment groups suggests that these agents activate molecular signaling pathways to accelerate the healing cascade long before macroscopic changes become apparent.

This study has some limitations. Firstly, the use of an acute, non–infected wound model limits the generalizability of the findings to more complex clinical scenarios, such as chronic or infected wounds. Secondly, the scope of the study is confined to the investigation of structural and cellular changes. Biomechanical tests, such as tensile strength measurement, which would determine whether the increased collagen deposition translates into a functional gain, were not included in this study. Such functional analyses are critical for complementing the clinical relevance of histological findings.

CONCLUSION

VetOzon and Madecassol are potent agents that significantly accelerate cutaneous wound healing compared to the natural repair process. The efficacy of the two agents stems from fundamentally different yet complementary mechanisms of action. Whereas VetOzon acts as a catalyst that initiates the healing cascade by triggering a controlled inflammatory response in the early phase, Madecassol functions as an anabolic stimulator that directly and prolongedly promotes the synthesis of a robust and mature extracellular matrix.

ACKNOWLEDGEMENT

Balikesir University Scientific Research Projects Coordinator (BAP) (No: 2017/195).

Conflicting interest

The authors have no conflicts of interest to declare.

BIBLIOGRAPHIC REFERENCES

[1] Reinke JM, Sorg H. Wound repair and regeneration. Eur. Surg. Res. [Internet]. 2012; 49(1):35–43. doi: https://doi.org/f3462m

[2] Gushiken LFS, Beserra FP, Bastos JK, Jackson CJ, Pellizzon CH. Cutaneous wound healing: An update from physiopathology to current therapies. Life [Internet]. 2021; 11(7):665. doi: https://doi.org/gpzjr3

[3] Sorg H, Tilkorn DJ, Hager S, Hauser J, Mirastschijski U. Skin wound healing: An update on the current knowledge and concepts. Eur. Surg. Res. [Internet]. 2017; 58(1–2):81–94. doi: https://doi.org/gh2dqr

[4] Peña OA, Martin P. Cellular and molecular mechanisms of skin wound healing. Nat. Rev. Mol. Cell Biol. [Internet]. 2024; 25(8):599–616. doi: https://doi.org/gt25gn

[5] Akita S. Wound repair and regeneration: Mechanisms, Signaling. Int. J. Mol. Sci. [Internet]. 2019; 20(24):6328. doi: https://doi.org/g7j69v

[6] Zhang Y, Lu Q. Immune cells in skin inflammation, wound healing, and skin cancer. J. Leukoc. Biol. [Internet]. 2024; 115(5):852–865. doi: https://doi.org/qmg2

[7] Rodrigues M, Kosaric N, Bonham CA, Gurtner GC. Wound healing: A cellular perspective. Physiol. Rev. [Internet]. 2019; 99(1):665–706. doi: https://doi.org/ghzzr5

[8] Tyavambiza C, Meyer M, Meyer S. Cellular and molecular events of wound healing and the potential of silver based nanoformulations as wound healing agents. Bioeng. [Internet]. 2022; 9(11):712. doi: https://doi.org/qmg4

[9] Yuliati L, Mardliyati E, Bramono K, Freisleben HJ. Asiaticoside induces cell proliferation and collagen synthesis in human dermal fibroblasts. Universa Med. [Internet]. 2015; 34(2):96–103. doi: https://doi.org/qgts

[10] Sun B, Wu L, Wu Y, Zhang C, Qin L, Hayashi M, Kudo M, Gao, M, Liu, T. Therapeutic potential of *Centella asiatica* and its triterpenes: a review. Front. Pharmacol. [Internet]. 2020; 11:568032. doi: https://doi.org/gpswgv

[11] Anzolin A, Da Silveira–Kaross N, Bertol C. Ozonated oil in wound healing: what has already been proven? Med. Gas Res. [Internet]. 2020; 10(1):54–59. doi: https://doi.org/gp7jx5

[12] Brito Júnior AAD, Carneiro JKMP, Reis JVNA, Oliveira TJS, Dantas JBDL. Application of ozonized oils in human body and oral cavity systems. RGO – Rev. Gaúch. Odontol. [Internet]. 2022; 70:e20220027. doi: https://doi.org/qmg5

[13] Ugazio E, Tullio V, Binello A, Tagliapietra S, Dosio F. Ozonated oils as antimicrobial systems in topical applications. their characterization, current applications, and advances in ımproved delivery techniques. Molecules [Internet]. 2020; 25(2):334. doi: https://doi.org/gkcf6q

[14] Cho K–H, Kim J–E, Bahuguna A, Kang D–J. Ozonated sunflower oil exerted potent anti–ınflammatory activities with enhanced wound healing and tissue regeneration abilities against acute toxicity of carboxymethyllysine in Zebrafish with ımproved blood lipid profile. Antioxidants [Internet]. 2023; 12(8):1625. doi: https://doi.org/qmg6

[15] Lim Y, Lee H, Woodby B, Valacchi G. Ozonated oils and cutaneous wound healing. Curr. Pharm. Des. [Internet]. 2019; 25(20):2264–2278. doi: https://doi.org/g9mvfw

[16] Ruiz–Vall A, Altamirano–Faus A, Bedmar–Gonzalez N, Andres–Lencina JJ. Improvement of surgical wound healing with ozonated oil in bilateral breast surgery: A pilot ıntra–patient comparative study. Cureus [Internet]. 2025; 17(6):e85829. doi: https://doi.org/qmg7

[17] Xiao W, Tang H, Wu M, Liao Y, Li K, Li L, Xu X. Ozone oil promotes wound healing by increasing the migration of fibroblasts via PI3K/Akt/mTOR signaling pathway. Biosci. Rep. [Internet]. 2017; 37(6):BSR20170658. doi: https://doi.org/fz27

[18] Ginel PJ, Negrini J, Guerra R, Lucena R, Ruiz–Campillo MT, Mozos E. Effect of topical ozonated sunflower oil on second intention wound healing in turtles: a randomised experimental study. J. Vet. Sci. [Internet]. 2021; 22(2):e27. doi: https://doi.org/qmg8

[19] Van De Vyver M, Boodhoo K, Frazier T, Hamel K, Kopcewicz M, Levi B, Maartens M, Machcinska S, Nunez J, Pagani C, Rogers E, Walendzik K, Wisniewska J, Gawronska–Kozak B, Gimble JM. Histology scoring system for murine cutaneous wounds. Stem Cells Dev. [Internet]. 2021; 30(23):1141–1152. doi: https://doi.org/gqp5b6

[20] Wilkinson HN, Hardman MJ. Wound healing: cellular mechanisms and pathological outcomes. Open Biol. [Internet]. 2020; 10(9):200223. doi: https://doi.org/gpqrtv

[21] Togi S, Togi M, Nagashima S, Kitai Y, Muromoto R, Kashiwakura J, Miura T, Matsuda T. Implication of NF–κB activation on ozone–ınduced HO–1 activation. BPB Rep. [Internet]. 2021; 4(2):59–63. doi: https://doi.org/qmg9

[22] Gunawan ES, Budiono BP. Enhancing the early inflammatory response: The role of ozonated *Aloe vera* oil on IL–6 and TNF–α in cutaneous wound repair. Biosci. Med. J. Biomed. Transl. Res. [Internet]. 2025; 9(9):2852–2865. doi: https://doi.org/qmhb

[23] Ozdemir O, Ozkan K, Hatipoglu F, Uyaroglu A, Arican M. Effect of asiaticoside, collagenase, and alpha–chymotrypsin on wound healing in rabbits. Wounds [Internet]. 2016 [cited Aug 20, 2025]; 28(8):279–286. Available in: https://goo.su/xq9Y

[24] Mamun AA, Shao C, Geng P, Wang S, Xiao J. Recent advances in molecular mechanisms of skin wound healing and its treatments. Front. Immunol. [Internet]. 2024; 15:1395479. doi: https://doi.org/g8qdxd

[25] Singh D, Rai V, Agrawal DK. Regulation of collagen I and collagen III in tissue injury and regeneration. Cardiol. Cardiovasc. Med. [Internet], 2023; 7(1):5–16. doi: https://doi.org/g86n33

[26] Budi EH, Schaub JR, Decaris M, Turner S, Derynck R. TGF–β as a driver of fibrosis: physiological roles and therapeutic opportunities. J. Pathol. [Internet]. 2021; 254(4):358–373. doi: https://doi.org/gphpf8

[27] Shi Z, Yao C, Shui Y, Li S, Yan H. Research progress on the mechanism of angiogenesis in wound repair and regeneration. Front. Physiol, 2023; 14:1284981. doi: https://doi.org/qmhc